Applied and Environmental Microbiology, Aug. 2008, p. 4782–4791 Vol. 74, No. 15
0099-2240/08/$08.00+0 doi:10.1128/AEM.01575-07

Esterase Autodisplay: Enzyme Engineering and Whole-Cell Activity Determination in Microplates with pH Sensors▽

Eva Schultheiss,[1] Svenja Weiss,[2] Elisa Winterer,[1] Ruth Maas,[1] Elmar Heinzle,[2] and Joachim Jose[1]*

Bioanalytics, Institute of Pharmaceutical and Medicinal Chemistry, Heinrich Heine University Düsseldorf, Universitätsstr. 1, 40225 Düsseldorf, Germany,[1] and Biochemical Engineering, Saarland University, P.O. Box 15 11 50, 66041 Saarbrücken, Germany[2]

Received 11 July 2007/Accepted 20 May 2008

Among the GDSL family of serine esterases/lipases is a group of bacterial enzymes that posses C-terminal extensions involved in outer membrane anchoring or translocation. ApeE from *Salmonella enterica* serovar Typhimurium, a member of this group, has been expressed in *Escherichia coli* and was resistant to protease digestion when the protease was added to whole cells, indicating a periplasmic localization. The five consensus blocks conserved within all GDSL esterases were identified in ApeE by multiple sequence alignment and separated from the C-terminal extension. The DNA sequence spanning the four invariant residues Ser, Gly, Asn, and His, and hence representing the catalytic domains of ApeE, was amplified by PCR and fused in frame to the transport domains of the autodisplay system. The resulting artificial esterase, called EsjA, was overexpressed in the cell envelope of *E. coli* and was shown to be active by the use of α-naphthyl acetate (α-NA) as a substrate in an in-gel activity stain after sodium dodecyl sulfate-polyacrylamide gel electrophoresis. Surface exposure of EsjA was indicated by its accessibility to protease added to whole cells. The esterase activity of whole cells displaying EsjA was determined by a pH agar assay and by the use of microplates with integrated pH-dependent optical sensors. α-NA, α-naphthyl butyrate, and α-naphthyl caproate were used as substrates, and it turned out that the substrate preferences of artificial EsjA were altered in comparison to original ApeE. Our results indicate that autodisplay of esterase in combination with pH sensor microplates can provide a new platform technology for the screening of tailor-made hydrolase activities.

Surface display of active proteins on living cells provides several advantages in biotechnological applications (26, 47). Using such cells as whole-cell biocatalysts, a substrate to be processed does not need to cross a membrane barrier but has free access. Moreover, being connected to a carrier (the cell as a biological matrix), the surface-displayed biocatalyst can be purified, stabilized, and applied to industrial processes more conveniently than it usually is as a free molecule. Using cellular surface display in creating and screening peptide or protein libraries to perform laboratory evolution has another benefit. By selecting the correct structure expressed at the surface, the corresponding gene, serving as an intrinsic label, is coselected and can be used in further studies and applications. Therefore, systems allowing the surface display of a maximum spectrum of different proteins are gaining growing importance in typical biochemical or bioorganic application fields, such as enzyme engineering or drug discovery (39).

In addition to other systems in bacteria and yeast (12, 13, 30, 43, 49), autodisplay is a very elegant way to express a recombinant protein on the surface of a gram-negative bacterium (26, 31). Autodisplay was developed based on the secretion mechanism of the autotransporter family of proteins (25). Recombinant passengers can be transported to the cell surface by simple insertion of the corresponding coding sequence into a distinct position of the transporter gene. Proteins expressed and transported as monomers can dimerize at the cell surface (22, 24, 27), which seems to be due to the particular anchoring mechanism within the cell envelope, which is mediated by a porin-like amphipathic β-barrel (32). It is possible to express enzymes in an active form at the cell surface; an inorganic prosthetic group can be inserted after surface translocation without loss of cell viability, and more than 1.8×10^5 molecules can be expressed on a single cell (24). Another advantage of autodisplay in biotechnological applications is the ability to use typical laboratory *Escherichia coli* strains as host organisms. Taking these facts together, autodisplay could be an interesting alternative to other systems dealing with the surface display of active proteins. Among these, the Lpp-OmpA surface display system and its derivatives seem to be the most effective, and they have been used successfully for the surface display of a wide variety of functional proteins and peptides, as well as random libraries of both in *E. coli* in the last decade (5, 8, 9, 15).

Esterases are a group of hydrolases that have wide substrate tolerances and are able to catalyze a broad spectrum of reactions even in organic solvents (6). Moreover, esterases show high regio- and/or enantioselectivity. They are not restricted to dissolving an ester bond but can also catalyze its formation and usually do not require any cofactors. Therefore, esterases in general are attractive tools for biocatalytic applications, such as chiral synthesis of pharmaceuticals or agrochemicals (17). Recently, several bacterial esterases have been subjected to laboratory evolution to obtain enzymes with improved properties, including substrate specificity or enantioselectivity (2, 33, 35). The primary aim of the present study was to combine the

* Corresponding author. Mailing address: Bioanalytics, Institute of Pharmaceutical and Medicinal Chemistry, Heinrich Heine University Düsseldorf, Universitätsstr. 1, D-40225 Düsseldorf, Germany. Phone: 49 211 811 3848. Fax: 49 211 811 3847. E-mail: joachim.jose@uni-duesseldorf.de.

▽ Published ahead of print on 30 May 2008.

advantages of cellular surface display with the attractive features of a bacterial esterase (4). Cellular esterase display would result in a whole-cell biocatalyst that should be easily applicable to industrial applications or organic synthesis processes (10). Moreover, it could serve as a starting point in a laboratory evolution approach, with no need for enzyme purification or the influence of different substrate accessibilities. A major bottleneck in the directed evolution of esterases, however, is the high-throughput enzyme activity determination (34). Either substrates containing chromophores have been used, which is a substantial constraint of the strategy, or highly sophisticated equipment, such as gas chromatography, mass spectroscopy, or high-performance liquid chromatography, has been applied, limiting the number of reactions determined within a certain period of time (3, 37, 41). Recently, we reported on a quantitative screening method for hydrolases by the use of microplates with integrated fluorochrome pH sensors (19, 20, 29). Therefore, a second aim of this study was to elucidate if this microplate assay could be used to determine the activity of esterase-displaying whole cells.

Here, we report on the surface display of an engineered esterase with high activity by the use of autodisplay in *E. coli*. Substrate conversion and specific activities were determined for three different substrates in microplates with integrated pH sensors.

MATERIALS AND METHODS

Bacterial strains, plasmids, and culture conditions. *E. coli* strain BL21(DE3) [F^- *ompT hsd*S_B(r_B^- m_B^-) *gal dcm* (DE3)] was used as the host strain for the expression of autotransporter fusion proteins. *E. coli* TOP10 [F′ *mcr*A Δ(*mrr-hsdRMS-mcrBC*) Φ80*lacZ*ΔM15 Δ*lacX74 recA1 deoR araD139* Δ(*ara-leu*)*7697 galU galK rpsL* (Str^r) *endA1 nupG*] and the vector pCR2.1-TOPO, which were used for subcloning of PCR products, were obtained from Invitrogen (Groningen, The Netherlands). Plasmid pCM343, which encodes esterase ApeE from *Salmonella enterica* serovar Typhimurium, has been described previously (7). Plasmid pETSH4, encoding the *a*dhesin *i*nvolved in *d*iffuse *a*dherence I (AIDA-I) autotransporter domains, including the 5 amino acids (PEYFK) that are recognized as a linear epitope by monoclonal antibody Dü142 under the control of the T7 promoter, has been further characterized elsewhere (28).

Bacteria were routinely grown at 37°C on Luria-Bertani (LB) agar plates containing 100 mg ampicillin per liter. For qualitative esterase determination with whole cells of *E. coli*, standard agar plates containing 1% agar were supplemented with 0.1% α-naphthyl acetate (α-NA) as a substrate and 0.01% bromcresol purple as a pH indicator (38). The substrate α-NA was first dissolved in methanol and kept as a 10% stock solution and was added after autoclaving of the agar solution immediately before the agar plates were poured. In addition, these agar plates contained 10 mM Tris/HCl, pH 7.0, for buffering. After inoculation with the different strains, the plates were incubated overnight at 37°C.

For differential cell fractionation and outer membrane preparations, flask cultures were carried out in 250-ml flasks containing 40 ml LB medium supplemented with 10 μM EDTA and 10 mM β-mercaptoethanol (24).

Recombinant DNA techniques. Plasmid pES02, which contains the artificial gene encoding the ApeE-autotransporter fusion protein, was constructed by PCR amplification using plasmid pCM343 (7) as a template and oligonucleotide primers esapeE5 (5′-GCTCTAGATTTGACTCTCTTACGGTGATT-3′) and esapeE6 (5′-GAAGATCTACGACTGCCTTGCGCCATCGACTG-3′). The amplified *apeE* gene is devoid of its own signal peptide and of its C-terminal part, which is responsible for membrane association. The amplified N-terminal part of *apeE* contains five blocks that are conserved among esterases of the GDSL type, as well as the catalytic triad (1), which was identified by sequence alignment of four esterase sequences (see Fig. 2). The PCR products derived from pCM343 by using *TaqZ*-polymerase (TaKaRa, Shiga, Japan) with the two primers esapeE05 and esapeE06 were digested with XbaI and BglII and ligated with the vector pCR2.1-TOPO, which had been digested before with the same enzymes. The *apeE* fragment was cut out by XbaI and BglII and ligated with pETSH4 cleaved with the same enzymes. Plasmid pETSH4 contains the genes coding for the AIDA-I autotransporter domains and the peptide antigen tag PEYFK under the control of an inducible T7 promoter (28). Insertion of the *apeE* PCR fragment yielded plasmid pES02, which encodes a fusion protein consisting of the signal peptide of pETSH4, truncated ApeE, the PEYFK epitope, and the AIDA-I autotransporter region, including a linker region that proved to be sufficient for full surface exposure (32) (see Fig. 3). The sequences of the PCR fragment and the ligation sites were controlled by DNA sequence analysis. All recombinant DNA techniques were performed according to standard procedures.

Differential cell fractionation and outer membrane preparation. Bacteria were grown overnight, and 1 ml of culture was used to inoculate 20 ml LB medium. For the expression of the autotransporter-esterase fusion protein FP89, cells were cultured at 37°C with vigorous shaking (200 rpm) until an optical density at 578 nm (OD_{578}) of 0.6 was reached and then induced with 1 mM IPTG (isopropyl-β-D-thiogalactoside) for 60 min. After the cells were harvested and washed with 0.2 M Tris/HCl, pH 8, differential cell fractionation was performed according to the method of Hantke (16) with modifications (38). Briefly, bacteria were incubated in a lysozyme solution (0.04-mg/ml final concentration) supplemented with 10 mM saccharose and 1 μM EDTA for 10 min at room temperature to lyse the cells. Then, aprotinin was added at a final concentration of 1 μg/ml, as well as 5 ml extraction buffer (2% Triton X-100, 50 mM Tris/HCl, 10 mM $MgCl_2$) and 0.1 mg DNase. After an incubation period of 30 min on ice, intact bacteria and large debris were sedimented by centrifugation at 1,600 × *g* for 5 min. The clarified bacterial lysate was centrifuged at 23,500 × *g* for 60 min, and the resulting supernatant, containing soluble cytoplasmic and periplasmic proteins, was completely aspirated. To resuspend the proteins, 10 ml phosphate-buffered saline (PBS) plus 1% sarcosyl (*N*-lauryl sarcosinate, sodium salt) was added, and the solution was once again centrifuged at 23,500 × *g* for 60 min. By this centrifugation step, the sarcosyl-soluble cytoplasmic membrane proteins contained in the supernatant could be separated from the pelleted outer membrane proteins. The pellet was washed twice with 10 ml of water, dissolved in 30 μl water, and prepared for sodium dodecyl sulfate-polyacrylamide gel electrophoresis (SDS-PAGE). To the soluble and cytoplasmic protein fractions, a fourfold volume of acetone was added, and samples were frozen for 1 h at −20°C. The precipitated proteins were obtained by centrifugation at 23,500 × *g* for 10 min, resuspended in water, and used for SDS-PAGE.

For whole-cell protease treatment, *E. coli* cells were harvested, washed, and resuspended in 5 ml 0.05 M Tris-HCl, 5 mM EDTA, 0.5% SDS, pH 7.8. To this cell suspension, 12 μl proteinase K stock solution was added to yield a final concentration of 50 μg protease ml^{-1}. The suspensions were incubated at 37°C for 60 min, and digestion was stopped by washing the cells three times with PBS containing 10% fetal calf serum. The outer membranes of digested cells were prepared as described above.

SDS-PAGE and Western blot analysis. Outer membrane isolates of *E. coli* cells expressing the esterase-autotransporter fusion protein were diluted 1:2 with sample buffer (100 mM Tris/HCl, pH 6.8) containing 4% SDS, 0.2% bromphenol blue, and 20% glycerol), boiled for 5 min, and analyzed on 12.5% acrylamide gels. For Western blot analysis, the gels were transferred onto polyvinylidene difluoride membranes, and the blotted membranes were placed in a blocking solution of 3% milk powder in PBS overnight. For immunodetection, the membranes were incubated with monoclonal antibody Dü142, recognizing the reporter epitope PEYFK, diluted 1:300 in PBS with 3% bovine serum albumin for 3 h. Dü142 was raised against the Nef protein of human immunodeficiency virus, was typed to recognize the linear epitope PEYFK, and was used for similar purposes in previous studies (14, 32). The immunoblots were washed three times with PBS prior to addition of the secondary antibody. Antigen-antibody conjugates were visualized by reaction with alkaline phosphatase-labeled goat anti-mouse immunoglobulin G secondary antibody (Kirkegaard & Perry Laboratories, Gaithersburg, MD) diluted 1:10,000 in PBS. A color reaction was achieved by incubating the immunoblots with *p*-nitroblue tetrazolium chloride (0.3 mg/ml, final concentration) and BCIP (5-bromo-4-chloro-3-indolyl phosphate, *p*-toluidine salt) (0.17 mg/ml, final concentration) in 100 mM Tris supplemented with 100 mM NaCl and 5 mM $MgCl_2$, pH 9.5.

Activity staining of SDS gels. After the SDS-PAGE proteins were renatured, activity staining was performed according to the method of Reiter et al. (36). Briefly, the gels were washed four times in 50 mM disodium hydrogen phosphate plus 12.5 mM citric acid, pH 6.3, for 30 min to remove SDS. To the first two washes, isopropanol was added to a final concentration of 25%. The gels were then soaked with α-NA solution (16 mg/ml acetone) and incubated for a maximum of 30 min at 37°C. Esterase-containing protein bands took on a dark-violet, almost black color in this procedure.

Microplate assay. The activity of whole cells was determined by a pH-dyn assay (46). In this way, the pH variation caused by the production of acids

generated by the hydrolysis of α-naphthyl esters was recorded. The pH variation was quantified by microplates with pH sensors, which were covalently immobilized at the bottom of each well (19). These sensor plates (PreSens, Regensburg, Germany) are common round-bottom 96-well polystyrene microplates. The optical sensor consists of an indicator fluorophore (carboxyfluorescein), which shows a pH-sensitive light emission, and an internal reference dye (sulforhodamine), which is insensitive to pH in its light emission (20). Excitation was at 492 nm for the indicator and 544 nm for the reference dye, and light emission was determined at 538 nm (indicator) and 590 nm (reference). Both compounds were covalently bound to the linear hydrogel polyhydroxyethylmethacrylate, a polymer that could be attached to the polystyrene surface of the microplate well. This ensured a constant ratio between the indicator and the reference dye and avoided elution of both compounds (20). For the determination of pH values, the light emission by the indicator and the reference dye at the corresponding wavelength was set to a ratio as described above. The relation between the pH and the ratio of the two emission intensities can be described by the Boltzman equation (46). For fluorescence measurement, a fluorescence intensity reader (BMG Fluostar, Germany) that is able to determine two wavelengths in parallel in one cycle was used.

For activity determination, 5 mM potassium phosphate buffer in 100 mM potassium chloride was used as a solvent. Low buffer concentrations are required in order to follow the alteration of the pH, depending on substrate hydrolysis. The additional potassium chloride is needed to provide the distinct ionic strength required for the immobilized sensor. The substrates applied were α-NA, α-naphthyl butyrate (α-NB), and α-naphthyl caproate (α-NC). They were dissolved in dimethyl sulfoxide and acetonitrile, with concentrations ranging from 80 to 200 mM. The volume in each well was 200 μl and consisted of 10 μl cell suspension (in phosphate buffer; corresponding OD_{660}, 0.25 to 0.5), 2 mM substrate, and phosphate buffer, resulting in a final concentration of dimethyl sulfoxide or acetonitrile of not more than 1 to 5%. Before activity determination was started, the buffer and cell suspension were mixed, and the alteration in pH was followed for 10 min. Subsequently, the reaction was started by addition of substrate solution, and values were taken every 90 seconds.

Substrate calculation. For a first screening of the enzyme activity of cells displaying EsjA on the surface, as well as for any other screening purpose, the curve giving the alteration in pH would be sufficient. In order to determine enzymatic activities in μmol/min, the pH values had to be converted to substrate or product courses. The pH curves could be converted into substrate concentrations via ion balances. An ion-charge balance could be noted as follows:

$$\sum_j([\text{cation}_j]\cdot z_j) = \sum_j([\text{anion}_j]\cdot z_j) \quad (1)$$

where the concentrations of all cations $[\text{cation}_j]$ and anions $[\text{anion}_j]$ are calculated from all strong and weak acids and bases in the assay, such as buffer, substrate, products, and cells. In the observed pH range, all strong acids and bases are completely dissociated (20). The concentration of dissociated weak acids and bases can be calculated by the following equation, with K_{a0} equal to 1:

$$[H_{n-L}A^{L-}] = \frac{[H^+]^{n-L}\cdot[A]_{tot}\cdot\prod_{q=0}^{L}K_{aq}}{\sum_{m=0}^{n}\left\{[H^+]^{n-m}\cdot\prod_{q=0}^{m}K_{aq}\right\}} \quad (2)$$

Here, n denotes the number of acid protons, H^+ is a proton, $H_{n-L}A^{L-}$ are anions of the acid H_nA, L is the number of dissociated protons, and K_{aq} is the different acidity constant for each species at the corresponding ionic strength (pK values: H_2O, 13.89; $H_2PO_4^-$, 2.04; HPO_4^{2-}, 6.87; PO_4^{3-}, 11.72; HAc, 4.64; HCO_3^-, 6.24; and CO_3^{2-}, 9.99) (20). For the calculation of the converted substrate concentrations from changes in pH, the MATLAB tool (Mathworks, Natick, MA) was used. The given parameters are buffer type and concentration, the pK_a values of all substances and species, the initial substrate concentration, and the four Boltzman constants for the calculation of pH from the intensity ratio.

RESULTS

Subcellular localization of ApeE from *S. enterica* serovar Typhimurium expressed in *E. coli*. ApeE from *Salmonella enterica* serovar Typhimurium was expressed in the OmpT-negative *E. coli* strain BL21(DE3) and subsequently subjected to SDS-PAGE analysis. For specific detection, the ApeE esterase was reactivated after SDS-PAGE. The ability to be reactivated is a characteristic feature of this enzyme and was described previously by Carinato et al. (7). In our experiments, it was used for in-gel activity staining and identification of the ApeE esterase band. By this method, in whole-cell lysates, as well as in outer membrane preparations obtained by differential cell fractionation, a band with an apparent molecular mass of 67 kDa was detectable, corresponding to the full-size ApeE esterase. As such, a band was not detectable in the cytoplasm fraction or in the inner membrane fraction; this indicated localization of the enzyme within the outer membrane, as proposed before (7). To elucidate whether the ApeE esterase is directed to the cell surface or to the periplasm, different proteases, including trypsin, proteinase K, thermolysin, and pig pancreatic elastase, were added to whole cells of *E. coli* expressing ApeE. The cell envelope does not allow proteins as large as these proteases to pass; therefore, digestion of ApeE would indicate its surface exposure. In none of the cases investigated was a reduction of molecular weight or a decrease in band staining intensity observed (Fig. 1). This pointed to a localization of the enzyme on the periplasmic face of the outer membrane. This is in concordance with the results obtained with EstE from *Xanthomonas vesicatoria*, a close homologue of ApeE, which has been shown to be located in the periplasm when expressed in *E. coli* (42). In this case, the protein was shown to be anchored within the outer membrane by the C terminus, forming a β-barrel, and the catalytic moiety was accessible only from the periplasmic side.

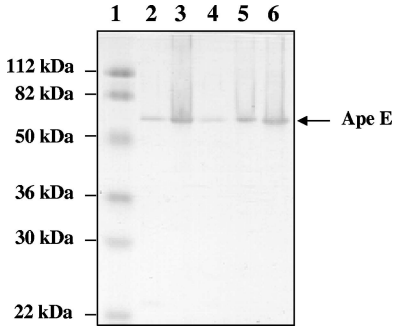

FIG. 1. Periplasmic localization of ApeE from *S. enterica* serovar Typhimurium expressed in *E. coli*. An in-gel esterase activity staining after SDS-PAGE is shown, as described in Materials and Methods. Lanes: 1, molecular mass marker; 2, whole-cell proteins of *E. coli* pCM343 expressing ApeE; 3, outer membrane proteins of *E. coli* pCM343; 4, whole-cell proteins of *E. coli* pCM343 prepared after 1 h of incubation of intact cells with proteinase K (50 μg ml^{-1}); 5, outer membrane proteins of *E. coli* pCM343 prepared after 1 h of incubation of intact cells with proteinase K (50 μg ml^{-1}); 6, outer membrane proteins of *E. coli* pCM343 prepared after 1 h of incubation of intact cells with proteinase K (100 μg ml^{-1}).

Multiple-sequence alignment and structure prediction. To investigate whether an organization similar to that found for EstE would match ApeE as well, multiple-sequence alignment of four bacterial esterases, ApeE; EstE, as mentioned above; EstA from *Pseudomonas aeruginosa* (48); and LipX from *Xenorhabdus luminescens* (45), was performed. As shown in Fig. 2, the five conserved blocks known to be characteristic of the

FIG. 2. Multiple-sequence alignment of ApeE from *S. enterica* serovar Typhimurium with LipX from *X. luminescens*, EstA from *P. aeruginosa*, and EstE from *X. vesicatoria*. The five blocks of amino acids that are characteristic of the GDSL family of hydrolases are highlighted with black boxes. The amino acids of the catalytic triad are marked by open triangles. The amino acid sequence corresponding to the DNA region that was amplified by PCR in order to construct the ApeE-autotransporter fusion protein (FP89) is bordered by black arrows. The GenBank accession numbers are as follows: AF047014 (ApeE), P40601 (LipX), AAB61674 (EstA), and AAP49127 (EstE). The multiple alignment was performed with the PileUp program of the GCG Wisconsin sequence analysis package using default values.

family of GDSL esterases (1), as well as the catalytic triad, were located within the first 350 amino acids of the complete 678-amino-acid-containing ApeE. Signal peptide cleavage was predicted by the SignalP program (11) to occur between A25 and F26, as was proposed earlier (7). The C-terminal part of ApeE was predicted to be comprised of 10 or 11 amphipathic β-sheets by using AMPHI, a protein structure prediction program that was successfully used before for the prediction of the structure of OmpF (18, 40, 44) and the autotransporter family of proteins (25). The prediction of such amphipathic β-sheets

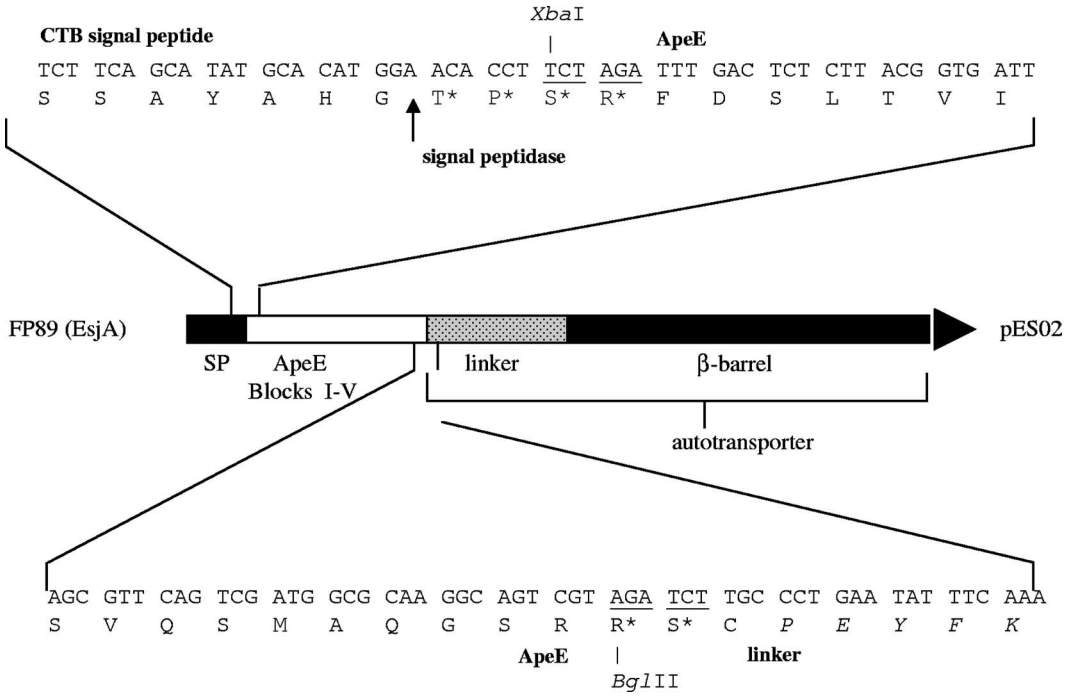

FIG. 3. Structure of the ApeE-autotransporter fusion protein FP89 encoded by plasmid pES02, constructed for autodisplay of esterase. The environment of the fusion sites is given as amino acid sequences. The signal peptidase cleavage site is indicated. The 4 amino acids at the N terminus and the 2 amino acids at the C terminus that were added laterally to the ApeE domains due to the cloning procedure are marked by asterisks. Restriction sites used for the insertion of the PCR product are underlined. The amino acids of a linear epitope of a monoclonal antibody that are part of the linker region and that were used for Western blot detection are written in italics. SP, signal peptide.

points to the formation of a β-barrel within the C-terminal part of ApeE, which could serve as an anchor within the outer membrane. All these findings are in complete congruence with those that were made earlier for EstE from *X. vesicatoria* (42). In summary, the ApeE esterase from *S. enterica* serovar Typhimurium is synthesized as a precursor protein, consisting of three domains. A signal peptide of 25 amino acids is located at the very N terminus, guiding the transport of the precursor across the inner membrane, and it is cleaved off, resulting in a reduction of the molecular mass of the precursor from 69.9 to 67 kDa, as has been described by Carinato et al. (7). In the N-terminal half, the mature protein contains the domains needed for esterase activity, and at the C-terminal end, it contains the domains that are supposed to be responsible for outer membrane anchoring. As ApeE esterase was not accessible to proteases added externally to whole cells when expressed in *E. coli*, this indicated a periplasmic orientation rather than a surface localization of the catalytic moiety.

Fusion of the catalytic domains of ApeE with the transport domains for autodisplay. Autodisplay exploits the signal peptide of the β-subunit of cholera toxin from *Vibrio cholerae* and the β-barrel, as well as the linker region of AIDA-I from enteropathogenic *E. coli* for transport of recombinant proteins to the cell surface (21, 31). In such cases, the encoding DNA sequence for the recombinant protein, the so-called passenger, must be inserted in frame between the coding sequence for the signal peptide and the coding sequence for the linker region (Fig. 3). By this strategy, a wide variety of proteins and peptides from different origins could be transported to the cell surfaces of *E. coli* and *Salmonella* (for an overview, see reference 21).

To confirm the distinct functional and structural arrangement of domains within mature ApeE as proposed in the preceding paragraph, we decided to transport the catalytic domains separately to the cell surface by autodisplay. For this purpose, a part of the coding region of ApeE was amplified by PCR, starting with F26 as the first amino acid of the mature enzyme and ending with R379, including the conserved blocks I to V and the catalytic triad (Fig. 2). The primers used for PCR added an XbaI restriction site at the 5′ end and a BglII site at the 3′ end that could be used for the in-frame insertion of the truncated ApeE gene within the autodisplay domains encoding segments (Fig. 3). The resulting plasmid was named pES02 and contained an artificial gene construct coding for a fusion protein comprised of the signal peptide of the β-subunit of cholera toxin; the catalytic domains of ApeE; and the linker region, including a peptide tag (PEYFK) for a mouse monoclonal antibody, as well as the β-barrel of AIDA-I for outer membrane translocation (28). The molecular mass of the fusion protein was predicted from the amino acid sequence to be 88.9 kDa, and therefore, it was named FP89.

Expression and subcellular localization of FP89, containing the catalytic domains of ApeE. Plasmid pES02, encoding FP89, was transformed into the OmpT-negative *E. coli* strain BL21(DE3), and gene expression was analyzed after induction with 1 mM IPTG for 1 h. For this purpose, the outer membranes were prepared from cells of BL21(DE3) without plasmid as a negative control, BL21(DE)(pES02), and BL21

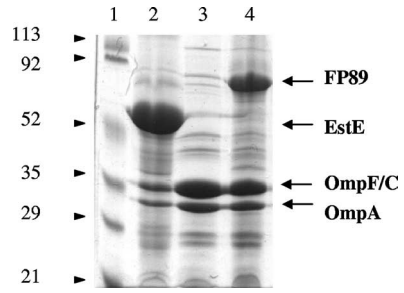

FIG. 4. Expression of fusion protein FP89 in *E. coli*. After induction for 1 h with 1 mM IPTG, outer membrane proteins were prepared from cells of *E. coli* BL21(DE3)(pMSEX9), encoding EstE from *X. vesicatoria* as a positive control (lane 2); BL21(DE3) without plasmid as a negative control (lane 3); and BL21(DE3)(pES02), expressing FP89 (EsjA, lane 4), and subjected to SDS-PAGE on a 12.5% polyacrylamide gel with subsequent Coomassie staining. Lane 1 shows the bands obtained by separation of the molecular weight standard; the corresponding molecular weights are given at the left. The natural outer membrane proteins of *E. coli*, OmpA and OmpF/C, which can be taken as an internal standard for the quantification of outer membrane proteins, are marked by arrows, as well as the bands corresponding to FP89 and EstE.

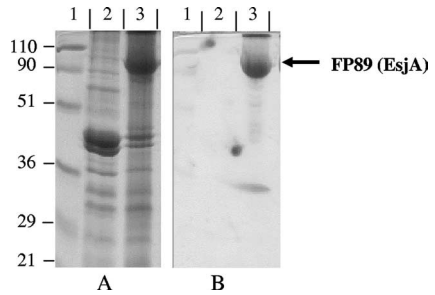

FIG. 5. SDS-PAGE (A) and in-gel activity staining (B) of outer membrane proteins prepared from cells of *E. coli* BL21(DE3)(pES02). In each panel, lane 1 shows the molecular weight standard and lane 2 shows the negative control, BL21(DE3) without plasmid, whereas lane 3 gives the results for *E. coli* BL21(DE3)(pES02). The staining of the FP89 band in panel B clearly indicates its esterase activity; therefore, it was renamed EsjA.

(DE3)(pMSEX9), encoding EstE from *X. vesicatoria*, as a positive control. As seen in Fig. 4, induction of BL21(DE3) cells containing pES02 with IPTG resulted in the strong expression of an 89-kDa protein, which was absent in BL21(DE3) cells. Expression of the artificial fusion protein was almost as strong as that observed for OmpA or OmpF/C, but not as strong as that observed for natural EstE expressed in *E. coli* (Fig. 4, lane 2). These results clearly indicated that combining the catalytic domains of ApeE with the transport domains for autodisplay resulted in an expressible fusion protein that was easily detectable within the outer membrane fraction of the corresponding *E. coli* cells by SDS-PAGE and subsequent Coomassie staining. No protein of 89 kDa was detectable in the cytoplasm fraction and the fraction representing the inner membrane proteins obtained after differential cell fractionation. Western blot analysis using the mouse monoclonal antibody against the peptide tag (PEYFK) introduced between the ApeE catalytic domains and the linker region of AIDA-I gave further proof of identity for FP89 (not shown), as it was clearly labeled in these experiments. No protein of a similar size was detectable in control cells, and no other cross-reactivity appeared. To find out whether FP89 was indeed bearing an ester-hydrolizing activity, an in-gel activity stain was performed, as described above for native ApeE and as has been reported by Carinato et al. (7) and Talker-Huiber et al. (42). Using α-NA as the substrate, which has been described as a suitable substrate for native ApeE, a dark-violet band became visible at the same position where FP89 was localized in SDS-PAGE or Western blot analysis (Fig. 5). This clearly indicated esterase activity of FP89. Therefore, we concluded that a new, "chimeric" esterase was constructed by genetic enzyme engineering, and it was termed EsjA.

For clarifying whether EsjA is directed toward the external side or the periplasmic side of the outer membrane, proteinase K was added to whole cells of *E. coli* BL21(DE) expressing the artificial enzyme. As mentioned above, proteinase K is not able to pass the outer membrane and enter the periplasm. Therefore, proteolytic degradation of a protein within the outer membrane after the addition of a protease to intact cells clearly indicates its surface exposure. As shown in Fig. 6, addition of proteinase K to whole cells of *E. coli* expressing EsjA resulted in the complete disappearance of the corresponding protein band, and no degradation products were detectable by Western blotting. This indicated that in EsjA, the catalytic domains are displayed at the cell surface, including at least that part of the linker region containing the peptide tag used for antibody binding. In consequence, autodisplay was applied successfully to direct a chimeric esterase that was engineered on the basis of ApeE from *S. enterica* serovar Typhimurium in a functional form to the cell surface of *E. coli*.

Esterase activity of whole cells of *E. coli* displaying EsjA. The formation of protons (or oxonium ions), which is closely correlated with substrate conversion by esterases, can be exploited for enzyme activity determination. In a first qualitative assay, we used agar plates containing bromcresol purple as a pH indicator dye and α-NA as a substrate in a manner similar to that described previously (38). *E. coli* BL21(DE3)(pES02) expressing EsjA, BL21(DE3)(pMSEX9) expressing EstE as a positive control, and BL21(DE3) cells without plasmid as a

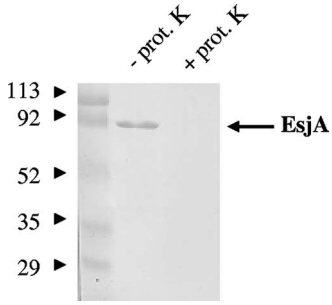

FIG. 6. Western blot of outer membrane proteins prepared from *E. coli* BL21(DE3)(pES02), treated with proteinase K (+ prot. K) or not (− prot. K). The protease was added to whole cells of *E. coli* for 60 min at 37°C, and subsequently, outer membrane proteins were prepared and subjected to SDS-PAGE on a 12.5% gel, followed by Western blotting. For detection, the monoclonal antibody against the linear epitope PEYFK (Fig. 3) was used.

FIG. 7. Agar plate pH assay. Bacteria from an overnight liquid culture were streaked out on agar plates containing 0.1% (wt/vol) α-NA as a substrate and 0.01% (wt/vol) bromcresol purple as a pH indicator. The inoculated agar plates were incubated overnight at 37°C. The cells applied were *E. coli* BL21(DE3)(pES02) expressing EsjA, *E. coli* BL21(DE3)(pMSEX9) expressing EstE from *X. vesicatoria*, and *E. coli* BL21(DE3) without plasmid as a negative control. Esterase activity of whole cells was indicated by the color of the agar changing from violet to yellow.

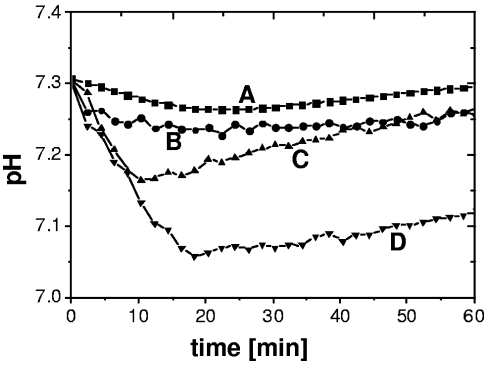

FIG. 8. Measurement of the conversion of α-NA to α-naphthol and acetate with pH sensor microplates. The assay was performed in 5 mM phosphate buffer, pH 7.3, and 5% DMSO. Lines: A (■), 2 mM α-NA, no cells added; B (●), *E. coli* BL21(DE3)(pES02) expressing EsjA, no α-NA added; C (▲), 2 mM α-NA, *E. coli* BL21(DE3); D (▼), 2 mM α-NA, *E. coli* BL21(DE3)(pES02) expressing EsjA. Each experiment was repeated at least three times independently, and each repetition resulted in similar curves.

negative control were plated out and incubated overnight at 37°C. Figure 7 shows that EsjA-displaying cells altered the color of the pH indicator from purple to yellow, clearly indicating acidification. Because this was not seen with control cells, it must have been due to the hydrolysis of the substrate α-NA and reflects the enzymatic activity of EsjA. The degree of yellow staining within the agar plate was in the same range as observed for the positive control EstE, which could be a hint that the fraction of active enzymes among all EsjA molecules expressed is in the same order of magnitude as found for EstE.

Whole-cell activity determination with pH sensor microplates. For further esterase activity determinations, a so-called pH-dyn method in 96-well microplates was used, as described previously (19, 20, 29). For this purpose, the change of pH depending on the hydrolysis of the substrate was determined by a pH-sensitive fluorescent dye that was integrated in the bottom of each microplate well.

In a first step, it was necessary to establish the appropriate test conditions in regard to (i) the applicable buffer system, (ii) the equitable substrate concentration, and (iii) the tolerated type of organic solvent, as well as the final concentration of organic solvent that was required for the substrate solution. For these experiments, α-NA was chosen, as it was converted as a substrate in the in-gel activity staining experiments described above. At this point, the poor solubility of α-naphthyl esters proved to be a major problem. In standard activity assays using α-NA as a substrate, the final assay concentration of dioxane, which was used for preparing the α-NA stock solution, was in the range of 20%. In our experiments, such a high concentration of dioxane destroyed the sensor and affected the polystyrene surface of the microplates. After assessing various types of organic solvents and solvent concentrations (not shown), suitable assay conditions were found, using dimethyl sulfoxide (DMSO) up to a final concentration of 5%. Optimal test conditions were determined to be 5 mM phosphate buffer with a starting pH of 7.4, 1 to 5% DMSO, and α-NA at a final concentration of 2 mM.

Subsequently, these conditions were used in an initial experiment to follow the alteration of pH by *E. coli* cells displaying EsjA in the wells of microplates with integrated pH sensors in comparison to different controls. As seen in curve D of Fig. 8, incubation of these cells with the substrate α-NA resulted in a clearly detectable and linear decrease in pH over a period of 20 min. The controls applied were cells displaying EsjA without substrate α-NA (curve B), cells with substrate α-NA but without EsjA displayed at the surface (curve C), and substrate α-NA without any type of cells (curve A). As shown in curve A, there was obviously a certain degree of autohydrolysis of α-NA, as manifested by a slight decrease in pH. The pH decrease in curve B of Fig. 8 is most likely caused by endogenous metabolism of *E. coli*, i.e., acid production without the addition of substrate and which is independent of any surface-displayed EsjA. It is important to note that the cells were not inactivated to avoid denaturation of the esterase, which would confound any screening purposes. In addition, it must be emphasized that a very low buffer concentration (5 mM Tris/HCl) was used, in order to be able to detect the pH shift caused by enzymatic activity. A low buffer concentration, in combination with living cells of *E. coli*, obviously resulted in the decrease in pH during the first 10 min of incubation. This type of endogenous metabolism was also found in cells displaying EsjA and cells displaying a control protein but not EsjA, but the detectable effect was terminated in every experiment after 10 min (Fig. 8, curve C). An explanation could be that this shift in pH during the first 10 min is due to degradation of an unknown intracellular compound that was accumulated before. Since all the cells were treated identically before incubation in the microplate, it is probable that all the cells accumulated in the same amount and needed the same time to secrete a related acid. Additionally, α-NA seems to have had a stimulating effect on the secretion of this compound. To elucidate this hypothesis, we performed identical experiments starting at different pH values in the

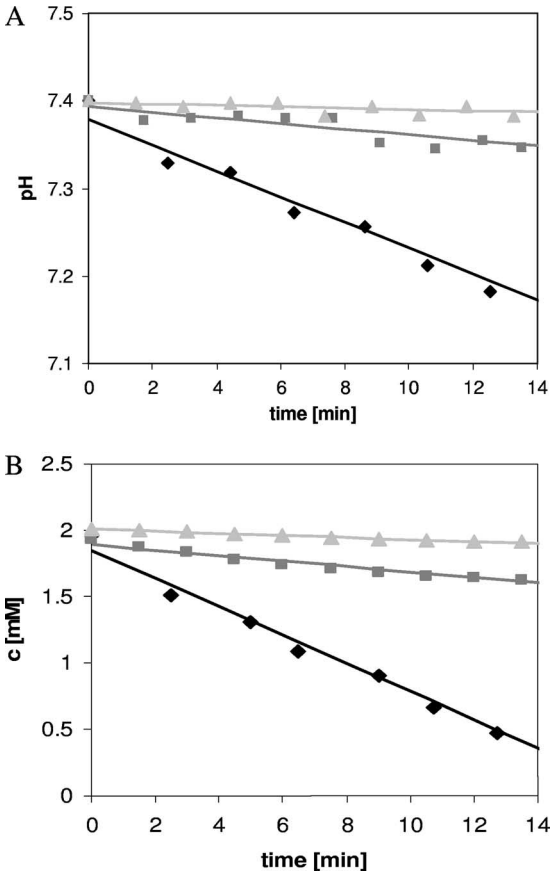

FIG. 9. Measurement of the conversion of 2 mM α-NA (◆), 2 mM α-NB (■), and 2 mM α-NC (▲) by *E. coli* BL21(DE3)(pES02) expressing EsjA at the cell surface with pH sensor microplates. The test conditions were as follows: 5 mM phosphate buffer, pH 7.4, 1% DMSO, 10 μl cell suspension (OD_{660}, 0.25) per well, 2 mM substrate per well. Each experiment was repeated at least three times independently, and each repetition resulted in similar curves. (A) Measured pH curves. The symbols give a selection of recorded pH values; the lines are the corresponding fitted data via spline interpolation. (B) Substrate conversion. The courses were calculated from the fitted pH curves in panel A.

range of 7.8 to 6.8, but in all of these experiments, a decrease in pH during the first 10 min was observed. As a consequence, we decided to start the determination of esterase activity in subsequent experiments after a 10-min preincubation with substrate. Nevertheless, at each reading point, the pH value obtained with controls cells was subtracted from the value obtained with cells displaying EsjA in order to calculate substrate conversion.

Hydrolytic activity of whole cells displaying EsjA toward α-NA, α-NB, and α-NC using microplate pH sensors. The specificities of whole cells displaying EsjA toward various substrates were compared by measuring the various pH courses in parallel using the sensor microplates with a microplate reader. α-NA, α-NB, and α-NC, which have been shown to be substrates of the egress esterase ApeE (Fig. 9A), were used as substrates. The highest rate of conversion was observed with α-NA. Application of α-NB and α-NC led to a clearly smaller pH decrease and indicated a lower conversion rate of these substrates by EsjA. The curves for all substrates appeared to be very similar; only weak differences in the initial slope were detectable. The measured pH courses were fitted via spline interpolation, and from these fitted curves, substrate concentrations were calculated using equation 1 combined with equation 2 (Fig. 9B). For this purpose, the pK_a values of all substrates, products, and buffer species had to be taken into account. The buffer capacities of the reference cells, as well as of the cells displaying EsjA, were negligible and were not included in the calculation. As shown in Fig. 9B, the calculated substrate curves are quite similar to the pH curves and represented enzyme activities in the range of 20 mU per well for the substrate α-NA. Because 10 μl of a cell suspension with an OD_{660} of 0.25 to 0.5 was added per well, and an OD_{660} of 0.1 corresponds to a cell number of 1×10^9, which was determined in a calibration curve (data not shown), this resulted in an enzyme activity of 1 unit per 0.13×10^8 to 0.25×10^8 cells of *E. coli* displaying EsjA toward α-NA. The activities of the identical cells toward α-NB and α-NC were significantly decreased. To our surprise, the substrate preferences of the whole cells displaying EsjA were different from those of egress ApeE enzyme from *S. enterica* serovar Typhimurium. For ApeE, the substrates most rapidly hydrolyzed were reported to be α-NB and α-NC (7). In our experiments with EsjA, α-NA was clearly the preferred substrate, followed by α-NB and α-NC.

DISCUSSION

Three important conclusions can be drawn from the present investigation. First, ApeE from *S. enterica* serovar Typhimurium is an esterase located in the outer membrane and anchored within by a C-terminal β-barrel. The catalytic domains are directed toward the periplasm, where they are protected from access by externally added proteases. Separating these catalytic domains from the β-barrel and fusing them to the transport domains of the autodisplay system resulted in the surface display of a highly active, "chimeric" esterase enzyme in *E. coli*.

This leads to the second important conclusion from this study, namely, that autodisplay is a tool for enzyme engineering and is applicable to the efficient surface display of engineered enzymes. The artificial fusion protein constructed thereby was named EsjA, and its expression was controlled by the inducible T7/Lac promoter within the pET vector backbone (23).

Two major differences were observed when comparing the chimeric esterase EsjA with the original ApeE expressed in *E. coli*. The first major difference is the remarkably increased substrate conversion of cells expressing EsjA in comparison to cells expressing the original ApeE. In our experiments, enzyme activity of ApeE was detectable only by in-gel activity staining; however, the activity of EsjA was also verifiable by an agar plate assay and by the microplate pH assay. No significant signals were obtained from cells expressing ApeE in these assays. Moreover, in contrast to the band obtained by the in-gel activity staining with EsjA, which was very intense (Fig. 5B, lane 3), the corresponding bands obtained with ApeE were faint (Fig. 1). This could be an indication that the difference in enzyme activities of cells expressing EsjA and cells expressing

ApeE is a result of the higher rate of expression obtained by the T7/Lac promoter in the pET vector system. This is supported by the results obtained by SDS-PAGE. Whereas EsjA was visible without problems as a prominent band by simple Coomassie brilliant blue staining (Fig. 4, lane 4, and Fig. 5A, lane 3), ApeE was hardly detectable as a very faint band in similar experiments. At this point, it must be emphasized that for all experiments referred to in this context, the ODs of cells, whether they expressed EsjA, ApeE, or even EstE, had been adjusted to identical values, indicating that we were dealing with similar numbers of cells in both cases. From these experiments, it can be concluded that the expression rate of EsjA is much higher than that of ApeE and, as consequence, that cells expressing EsjA exhibit higher substrate conversion rates than those expressing ApeE. However, these experiments are not suitable to exclude any difference in specific activities between the two enzyme molecules.

This notion is particularly accentuated by the second difference between the two enzymes ApeE and EsjA, namely, the difference in substrate preferences (Fig. 9). This could be an indication that the fusion of the catalytic domains of ApeE to the transport domains of autodisplay has a considerable effect on the structure of the resulting biocatalyst and that this can lead to altered enzyme activities toward a given set of substrates. A similar observation was made earlier with the surface display of sorbit dehydrogenase (SDH) from *R. sphaeroides* using the autodisplay system in *E. coli* (27). In contrast to purified SDH, which converted sorbitol at the highest rates and then galactitol, followed by arabitol, the enzyme displayed on the cell surface of *E. coli* preferred arabitol as a substrate, followed by sorbitol and galactitol. Theoretically, at least for the esterase, it is also possible that the altered substrate preferences could be affected by the localization of the catalytic domain —the periplasmic face of the outer membrane in the case of ApeE and the outer face of the outer membrane in the case of EsjA. This situation is not a principal obstacle in using an artificial or engineered esterase enzyme like EsjA or the surface-displayed SDH for biotechnological purposes. However, it clearly indicates that data obtained with such an artificial system cannot be transferred blindly to the natural situation.

Finally, the third important conclusion that can be drawn from this investigation is that the esterase activities of whole cells displaying EsjA could be measured in a microplate pH assay without the need for cell disruption or any further preparation steps. In particular, this can be important if an enzyme is sought for the conversion of a large substrate that is unable to cross the membrane barrier. In addition, by combining the surface display of an esterase with the microplate pH assay, a novel tool for the screening of novel hydrolytic enzymes is obtained and can be provided for laboratory evolution approaches.

ACKNOWLEDGMENTS

We are grateful to C. G. Miller for the gift of plasmid pCM343.

The Deutsche Bundesstiftung Umwelt provided financial support (AZ 13040/15).

REFERENCES

1. **Akoh, C. C., G. C. Lee, Y. C. Liaw, T. H. Huang, and J. F. Shaw.** 2004. GDSL family of serine esterases/lipases. Prog. Lipid Res. **43:**534–552.
2. **Akoh, C. C., G. C. Lee, and J. F. Shaw.** 2004. Protein engineering and applications of *Candida rugosa* lipase isoforms. Lipids **39:**513–526.
3. **Becker, S., A. Michalczyk, S. Wilhelm, K. E. Jaeger, and H. Kolmar.** 2007. Ultrahigh-throughput screening to identify *E. coli* cells expressing functionally active enzymes on their surface. Chembiochem **8:**943–949.
4. **Becker, S., S. Theile, N. Heppeler, A. Michalczyk, A. Wentzel, S. Wilhelm, K. E. Jaeger, and H. Kolmar.** 2005. A generic system for the *Escherichia coli* cell-surface display of lipolytic enzymes. FEBS Lett. **579:**1177–1182.
5. **Bessette, P. H., J. J. Rice, and P. S. Daugherty.** 2004. Rapid isolation of high-affinity protein binding peptides using bacterial display. Protein Eng. Des. Sel. **17:**731–739.
6. **Bornscheuer, U. T.** 2002. Microbial carboxyl esterases: classification, properties and application in biocatalysis. FEMS Microbiol. Rev. **26:**73–81.
7. **Carinato, M. E., P. Collin-Osdoby, X. Yang, T. M. Knox, C. A. Conlin, and C. G. Miller.** 1998. The *apeE* gene of *Salmonella typhimurium* encodes an outer membrane esterase not present in *Escherichia coli*. J. Bacteriol. **180:**3517–3521.
8. **Dane, K. Y., L. A. Chan, J. J. Rice, and P. S. Daugherty.** 2006. Isolation of cell specific peptide ligands using fluorescent bacterial display libraries. J. Immunol. Methods **309:**120–129.
9. **Daugherty, P. S., B. L. Iverson, and G. Georgiou.** 2000. Flow cytometric screening of cell-based libraries. J. Immunol. Methods **243:**211–227.
10. **Drepper, T., T. Eggert, W. Hummel, C. Leggewie, M. Pohl, F. Rosenau, S. Wilhelm, and K. E. Jaeger.** 2006. Novel biocatalysts for white biotechnology. Biotechnol. J. **1:**777–786.
11. **Emanuelsson, O., S. Brunak, G. von Heijne, and H. Nielsen.** 2007. Locating proteins in the cell using TargetP, SignalP and related tools. Nat. Protoc. **2:**953–971.
12. **Francisco, J. A., and G. Georgiou.** 1994. The expression of recombinant proteins on the external surface of *Escherichia coli*. Biotechnological applications. Ann. N. Y. Acad. Sci. **745:**372–382.
13. **Georgiou, G., C. Stathopoulos, P. S. Daugherty, A. R. Nayak, B. L. Iverson, and R. Curtiss III.** 1997. Display of heterologous proteins on the surface of microorganisms: from the screening of combinatorial libraries to live recombinant vaccines. Nat. Biotechnol. **15:**29–34.
14. **Gombert, F. O., R. Schaude, W. Troeger, G. Jung, B. H. W. Ruebsamen-Waigmann, S. Pfeifer, K. Krohn, M. Taehtinen, V. Ovod, A. Ranki, L. Shi, and P. Wernet.** 1990. Complete epitope fine-mapping of HIV-1 Nef-protein, p. 827–875. *In* E. Giralt and D. Andreu (ed.), Peptides. Escom Science Publishers, Leiden, The Netherlands.
15. **Hall, S. S., S. Mitragotri, and P. S. Daugherty.** 2007. Identification of peptide ligands facilitating nanoparticle attachment to erythrocytes. Biotechnol. Prog. **23:**749–754.
16. **Hantke, K.** 1981. Regulation of ferric iron transport in *Escherichia coli* K12: isolation of a constitutive mutant. Mol. Gen. Genet. **182:**288–292.
17. **Jaeger, K. E., and M. T. Reetz.** 1998. Microbial lipases form versatile tools for biotechnology. Trends Biotechnol. **16:**396–403.
18. **Jahnig, F.** 1990. Structure predictions of membrane proteins are not that bad. Trends Biochem. Sci. **15:**93–95.
19. **John, G. T., D. Goelling, I. Klimant, H. Schneider, and E. Heinzle.** 2003. pH-sensing 96-well microtitre plates for the characterization of acid production by dairy starter cultures. J. Dairy Res. **70:**327–333.
20. **John, G. T., and E. Heinzle.** 2001. Quantitative screening method for hydrolases in microplates using pH indicators: determination of kinetic parameters by dynamic pH monitoring. Biotechnol. Bioeng. **72:**620–627.
21. **Jose, J.** 2006. Autodisplay: efficient bacterial surface display of recombinant proteins. Appl. Microbiol. Biotechnol. **69:**607–614.
22. **Jose, J., R. Bernhardt, and F. Hannemann.** 2002. Cellular surface display of dimeric Adx and whole cell P450-mediated steroid synthesis on *E. coli*. J. Biotechnol. **95:**257–268.
23. **Jose, J., and S. Handel.** 2003. Monitoring the cellular surface display of recombinant proteins by cysteine labeling and flow cytometry. Chembiochem **4:**396–405.
24. **Jose, J., F. Hannemann, and R. Bernhardt.** 2001. Functional display of active bovine adrenodoxin on the surface of *E. coli* by chemical incorporation of the [2Fe-2S] cluster. Chembiochem **2:**695–701.
25. **Jose, J., F. Jahnig, and T. F. Meyer.** 1995. Common structural features of IgA1 protease-like outer membrane protein autotransporters. Mol. Microbiol. **18:**378–380.
26. **Jose, J., and T. F. Meyer.** 2007. The autodisplay story, from discovery to biotechnical and biomedical applications. Microbiol. Mol. Biol. Rev. **71:**600–619.
27. **Jose, J., and S. von Schwichow.** 2004. Autodisplay of active sorbitol dehydrogenase (SDH) yields a whole cell biocatalyst for the synthesis of rare sugars. Chembiochem **5:**100–108.
28. **Jose, J., and S. von Schwichow.** 2004. "Cystope tagging" for labeling and detection of recombinant protein expression. Anal. Biochem. **331:**267–274.
29. **Kumar, S., C. Wittmann, and E. Heinzle.** 2004. Minibioreactors. Biotechnol. Lett. **26:**1–10.
30. **Lee, S. Y., J. H. Choi, and Z. Xu.** 2003. Microbial cell-surface display. Trends Biotechnol. **21:**45–52.
31. **Maurer, J., J. Jose, and T. F. Meyer.** 1997. Autodisplay: one-component

system for efficient surface display and release of soluble recombinant proteins from *Escherichia coli*. J. Bacteriol. **179:**794–804.
32. **Maurer, J., J. Jose, and T. F. Meyer.** 1999. Characterization of the essential transport function of the AIDA-I autotransporter and evidence supporting structural predictions. J. Bacteriol. **181:**7014–7020.
33. **Reetz, M. T.** 2000. Evolution in the test tube as a means to create enantioselective enzymes for use in organic synthesis. Sci. Prog. **83:**157–172.
34. **Reetz, M. T., and L. W. Wang.** 2006. High-throughput selection system for assessing the activity of epoxide hydrolases. Comb. Chem. High Throughput Screen. **9:**295–299.
35. **Reetz, M. T., S. Wilensek, D. Zha, and K. E. Jaeger.** 2001. Directed evolution of an enantioselective enzyme through combinatorial multiple-cassette mutagenesis. Angew. Chem. Int. Ed. Engl. **40:**3589–3591.
36. **Reiter, B., A. Glieder, D. Talker, and H. Schwab.** 2000. Cloning and characterization of EstC from *Burkholderia gladioli*, a novel-type esterase related to plant enzymes. Appl. Microbiol. Biotechnol. **54:**778–785.
37. **Schmidinger, H., R. Birner-Gruenberger, G. Riesenhuber, R. Saf, H. Susani-Etzerodt, and A. Hermetter.** 2005. Novel fluorescent phosphonic acid esters for discrimination of lipases and esterases. Chembiochem **6:**1776–1781.
38. **Schultheiss, E., C. Paar, H. Schwab, and J. Jose.** 2002. Functional esterase surface display by the autotransporter pathway in *Escherichia coli*. J. Mol. Catal. B **18:**89–97.
39. **Sergeeva, A., M. G. Kolonin, J. J. Molldrem, R. Pasqualini, and W. Arap.** 2006. Display technologies: application for the discovery of drug and gene delivery agents. Adv. Drug Deliv. Rev. **58:**1622–1654.
40. **Surrey, T., A. Schmid, and F. Jahnig.** 1996. Folding and membrane insertion of the trimeric beta-barrel protein OmpF. Biochemistry **35:**2283–2288.
41. **Susani-Etzerodt, H., H. Schmidinger, G. Riesenhuber, R. Birner-Gruenberger, and A. Hermetter.** 2006. A versatile library of activity-based probes for fluorescence detection and/or affinity isolation of lipolytic enzymes. Chem. Phys. Lipids **144:**60–68.
42. **Talker-Huiber, D., J. Jose, A. Glieder, M. Pressnig, G. Stubenrauch, and H. Schwab.** 2003. Esterase EstE from *Xanthomonas vesicatoria* (Xv_EstE) is an outer membrane protein capable of hydrolyzing long-chain polar esters. Appl. Microbiol. Biotechnol. **61:**479–487.
43. **Ueda, M., and A. Tanaka.** 2000. Genetic immobilization of proteins on the yeast cell surface. Biotechnol. Adv. **18:**121–140.
44. **Vogel, H., and F. Jahnig.** 1986. Models for the structure of outer-membrane proteins of *Escherichia coli* derived from raman spectroscopy and prediction methods. J. Mol. Biol. **190:**191–199.
45. **Wang, H., and B. C. Dowds.** 1993. Phase variation in *Xenorhabdus luminescens*: cloning and sequencing of the lipase gene and analysis of its expression in primary and secondary phases of the bacterium. J. Bacteriol. **175:**1665–1673.
46. **Weiss, S., G. T. John, I. Klimant, and E. Heinzle.** 2002. Modeling of mixing in 96-well microplates observed with fluorescence indicators. Biotechnol. Prog. **18:**821–830.
47. **Wernerus, H., and S. Stahl.** 2004. Biotechnological applications for surface-engineered bacteria. Biotechnol. Appl. Biochem. **40:**209–228.
48. **Wilhelm, S., J. Tommassen, and K. E. Jaeger.** 1999. A novel lipolytic enzyme located in the outer membrane of *Pseudomonas aeruginosa*. J. Bacteriol. **181:**6977–6986.
49. **Yeung, Y. A., and K. D. Wittrup.** 2002. Quantitative screening of yeast surface-displayed polypeptide libraries by magnetic bead capture. Biotechnol. Prog. **18:**212–220.